Selectively Swollen Films of Triblock/Diblock Copolymer Blends: Dependence of Swollen Film Structure on Blend Composition

Rastislav Levicky,† Nagraj Koneripalli,‡ and Matthew Tirrell*

Department of Chemical Engineering and Materials Science, University of Minnesota, Minneapolis, Minnesota 55455

John F. Ankner and Helmut Kaiser

Missouri University Research Reactor, Columbia, Missouri 65211

Sushil K. Satija

NIST Center for Neutron Research, Gaithersburg, Maryland 20899

Received November 3, 1997; Revised Manuscript Received April 16, 1998

ABSTRACT: Compositional variation in blends of triblock and diblock copolymer films can be used to adjust the film response to a selective solvent. We investigated the relationship between blend composition and film structure in ordered films containing poly(styrene-*b*-2-vinylpyridine) (PS−P2VP) diblocks and PS−P2VP−PS triblocks. The study focuses on films possessing a lamellar morphology. Methanol, a strongly selective solvent for P2VP, is used to swell the films. Since methanol solvates P2VP but not PS, periodic multilayer structures result in which solvent-rich P2VP domains are separated by undissolved PS domains. The film structure is characterized in the dry and swollen states with neutron reflectivity. Although the dry state morphology dimensions are practically identical for all samples, in the swollen state films richer in triblock swell less due to higher density of bridges interconnecting the PS domains. Furthermore, in swollen triblock-containing samples, polymer concentration variations in P2VP domains are suppressed and the PS domains are better aligned with respect to the substrate.

1. Introduction

Chain architecture plays an important role in determining the properties of block copolymer systems. If three or more blocks are present on a linear block copolymer, the "middle" blocks can form bridges between the different domains that exist in the microphase separated state. On the other hand, end blocks can only form dangling tails. These points are illustrated in Figure 1, which depicts lamellar triblock and diblock films. In the diblock film, only tails are present while in the triblock film the middle blocks form either bridges or loops. The presence of bridges allows triblocks and higher order multiblocks to organize into networks, leading to technologically important materials such as thermoplastic elastomers.[1] In applications of block copolymers as surface modifiers, triblocks can lead to bridging-induced attraction between a pair of surfaces adsorbing for the end-blocks.[2,3] Other important properties, such as the location of the order to disorder transition,[4,5] are also affected by the number and distribution of blocks. These select examples illustrate that control over chain architecture can serve an important regulatory function in many practical situations using block copolymers.

Chain architecture and the presence of bridges also affect the response of ordered block copolymer systems to a selective solvent. A selective solvent cannot dissolve all of the domains in a block copolymer microstructure, swelling some domains while others are left undissolved.

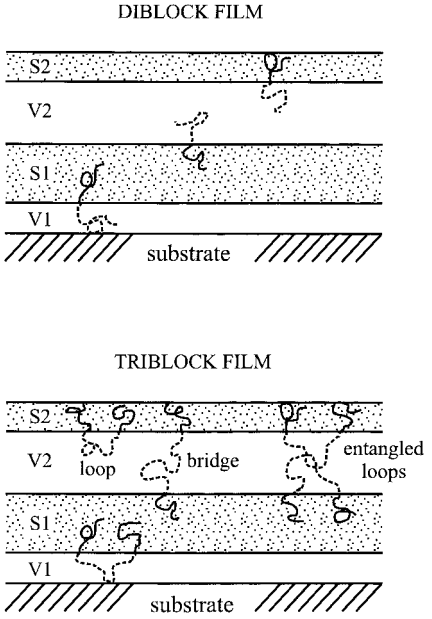

Figure 1. Structure of lamellar, 1.5 bilayers thick diblock, and triblock films. In the triblock film, single chain and entangled loop bridges are present whereas in the diblock both blocks form tails. The individual domains have been labeled for later reference.

Since bridging effectively cross-links the specimen, selectively swollen triblock or higher order multiblock structures have been termed "mesogels" in the literature.[6,7] While selectively swollen triblock films do not appear to have been previously investigated, several reports address selectively swollen bulk triblock systems.[8−10] For example, shear-ordered poly(styrene)−poly(butadiene)−poly(styrene) specimens were exposed

* To whom correspondence should be addressed.
† Present address: National Institute of Standards and Technology, Bldg. 221/A303, Gaithersburg, MD 20899.
‡ Present address: 3M Corporate Research Science Research Laboratory, 201-2N-19 3M Center, St. Paul, MN 55144.

S0024-9297(97)01618-5 CCC: $15.00
Published on Web 07/03/1998

Table 1. Block Copolymer Characteristics[a]

polymer	M_n (10^3 g/mol)	M_w/M_n	f_{P2VP}	N_{P2VP}	N_{PS}
PS−P2VP	78	1.06	0.50	390	360
PS−P2VP−PS	159	1.13	0.50	790	730

[a] M_n and M_w are the number and weight average molecular weights; f_{P2VP} is the volume fraction of P2VP; N_i is the number of type i monomers.

to hydrocarbon vapors by Folkes and Keller.[9] In this case, the solvent was selective for poly(butadiene) domains. The authors reported anisotropic swelling in lamellar and cylindrical morphologies. In lamellar samples, swelling up to ∼30% was observed to be reversible. Reynders et al.[10] studied spherical mesogels under an imposed uniaxial load and characterized the accompanying structural rearrangements by examining neutron scattering patterns. Depending on the block copolymer architecture and the ratio of polymer to solvent, an affine or a more complex structural deformation was observed in accordance with the network nature of the specimens. These and other studies demonstrated the influence of bridging and chain architecture on the behavior of bulk triblock systems in the presence of solvents.

In this article, we investigate the selective swelling of lamellar poly(styrene-*b*-2-vinylpyridine) (PS−P2VP) diblock and PS−P2VP−PS triblock films. Methanol, a good solvent for P2VP but a nonsolvent for PS, causes a pronounced swelling of the P2VP domains while leaving the PS domains undissolved. An important question we wish to examine is how the film response to a selective solvent can be adjusted in blend films that contain both triblock and diblock components. The film composition, and therefore the extent of bridging, is varied between the pure triblock and the pure diblock limits. We also provide details on the structure of swollen films, such as the distribution of polymer within swollen P2VP domains and the possibility of bridge relaxation. Neutron reflectivity is used to depth-profile the sample structure in the dry and swollen states.

After outlining the experimental techniques and data analysis in section 2, we present the neutron reflectivity data and fits at the beginning of section 3. Here we also consider issues such as the effects of repeated cycling between swollen and dry states. Next, we discuss the details of the sample structure including the dependence of swollen film dimensions on triblock fraction. We conclude by summarizing the main points in section 4.

2. Experimental Section

Sample Preparation. The 159K (K = 10^3 g/mol) PS−P2VP−PS triblock and 78K PS−P2VP diblock copolymers were anionically synthesized and characterized as described elsewhere.[11] Their molecular characteristics are listed in Table 1. None of the blocks were deuterated. Films of the block copolymers were spin-coated from a toluene solution (∼1.5% w/v) onto polished, ⟨111⟩ silicon wafer disks 100 mm in diameter and 13 mm thick. Immediately prior to spin coating, the silicon wafer substrates were cleaned for 10 min in 120 °C "piranha" solution (3:7 mixture of aqueous (30%) hydrogen peroxide and concentrated sulfuric acid), rinsed with 18 MΩ cm water, and dried under a nitrogen stream. *WARNING! Piranha solution reacts violently with organics and must not be stored in tightly sealed containers.* The spin coating was performed at about 2000 rpm, producing films close to 600 Å thick. This thickness corresponds to 1.5 bilayers of block copolymer as illustrated in Figure 1. Samples were prepared with 0, 20%, 50%, 80%, and 100% volume fraction of triblock. The spin-coated films were annealed under vacuum for 5 days at 185 °C to order the film morphology into lamellae parallel to the substrate. All annealed films were checked under an optical microscope to ascertain that less than 5% surface coverage of islands or holes[12] was present. Such topographical features arise if the spin-coated thickness is incommensurate with the $[n + {}^1/_2]D$ film thickness quantization (n = integer, D = thickness of one bilayer) originating from interfacial wetting preferences. The minimization of surface topography facilitated the analysis of neutron reflectivity data.

Neutron Reflectivity Measurements and Analysis. Neutron reflectivity measurements were conducted at the Missouri University Research Reactor (MURR), Columbia, MO, and at the National Institute of Standards and Technology (NIST), Gaithersburg, MD. The fraction of neutrons reflected off the sample, termed the reflectivity R, was obtained as a function of the momentum transfer $q_z = 4\pi \sin(\theta)/\lambda$. θ is the angle between the sample surface and the incident beam and λ is the wavelength of the neutrons (MURR, $\lambda = 2.35$ Å; NIST, $\lambda = 4.77$ Å). Since the instruments operate at fixed wavelength, q_z was varied by changing θ. Background scattering was measured by offsetting the detector with respect to the specular scattering direction. Prior to analysis, all data were background corrected and normalized to the incident beam intensity. The instrumental resolution $\Delta q_z/q_z$ (hwhm of a Gaussian spread) was constant over the experimental q_z range ($0.005 \le q_z \le 0.1$ Å^{-1}) and was close to 0.027 for all data.

The experiments were conducted in temperature-controlled solvent cells,[11] at a temperature of 27 ± 1 °C. After the reflectivity was measured from the dry film, the cell was filled with methanol and allowed to stand at least 8 h before solvent data were collected. Either unlabeled CH_3OH or perdeuterated CD_3OD methanol was used. The attainment of swelling equilibrium was individually checked for each solvent scan by rerunning the lower half of the q_z range at least 4 h later (prior to drying the sample). In all cases, it was confirmed that the two curves superposed so that no detectable changes were occurring over this time scale. A sample was dried by draining the solvent and flowing nitrogen gas through the cell for 10 min. We note that the neutron beam was incident through the silicon wafer substrate, reflected off the wafer/polymer film/solvent interface, and exited through the other side of the wafer.

Neutron reflectivity data were analyzed by determining a sample structure consistent with the experimental R vs q_z curve. The details of such procedures can be found elsewhere.[11,13,14] Briefly, the reflectivity is calculated for a series of trial sample structures and compared to the experimental data. The goodness of fit is judged by a χ^2 statistic.[15] The sample structure is represented by its scattering length density (SLD) profile, which is related to the sample composition via

$$\mathrm{SLD}(z) = \sum_i \Phi_i(z)\mathrm{SLD}_i$$

where $\Phi_i(z)$ is the volume fraction of species i a distance z from the substrate and SLD_i is its scattering length density. We generated trial SLD profiles in two ways: (1) through a piecewise model where each layer (PS or P2VP) was represented by a box or a simple polynomial function and the interfaces between layers were smoothed by Gaussian convolution, or (2) via a cubic spline expansion following the approach of Pedersen.[16] The structural model approach (1) requires fewer parameters, and the SLD profile can be constrained to possess only anticipated features; on the other hand, the cubic spline representation is very flexible and well suited to suggesting additional structural features necessary to improve the fit. Thus, the data were often analyzed by first fitting a box model to extract the values of the most important parameters such as domain widths and then using them as an initial guess for the spline algorithm to determine further refinements. The SLD was discretized into 2 or 3 Å thick slabs, and a recursion algorithm[13,14] was applied to calculate the reflectivity. For all box function models, mass conservation was enforced by performing the dry sample fits first and using

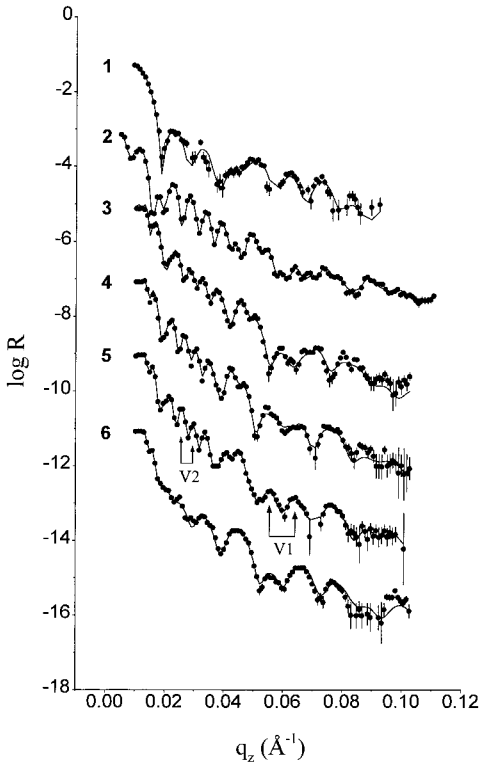

Figure 2. Reflectivity data (●) and calculated fits (—) for **(1)** 50% triblock film in the dry state, **(2)** 100% triblock film under CH_3OH, **(3)** 80% triblock film under CD_3OD, **(4)** 50% triblock film under CD_3OD, **(5)** 20% triblock film under CD_3OD, and **(6)** 0% triblock film under CD_3OD. The data have been vertically offset. The arrows on the 20% triblock data (curve 5) indicate the approximate domain width to which the interference fringes correspond.

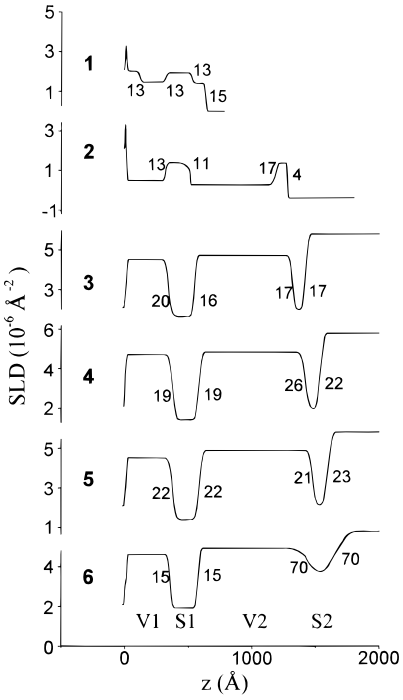

Figure 3. Scattering length density profiles derived from the data in Figure 2: **(1)** 50% triblock sample in the dry state, **(2)** 100% triblock under CH_3OH, **(3)** 80% triblock under CD_3OD, **(4)** 50% triblock under CD_3OD, **(5)** 20% triblock under CD_3OD, and **(6)** 0% triblock under CD_3OD. The swollen profiles correspond to the initial swelling of the films and were generated using box function models. The SLD of P2VP domains is greater than that of the PS domains in the dry or CD_3OD swollen states, while the opposite applies to CH_3OH swollen films. The numbers next to interfaces give the root-mean-square interfacial widths in Å (the individual interfacial widths have about a ±20% uncertainty).

them to fix the amount of polymer in a PS or P2VP domain in the presence of solvent. Although material conservation was not enforced in the cubic spline algorithm, this condition was obeyed to better than 10% variation in the amount of polymer.

Perdeuterated methanol, CD_3OD, was employed to enhance the contrast between P2VP and the solvent (P2VP, SLD = 2.0×10^{-6} Å^{-2}; CD_3OD, SLD = 5.8×10^{-6} Å^{-2}; CH_3OH, SLD = -0.37×10^{-6} Å^{-2}). The enhanced contrast was exploited to determine additional detail in the SLD profiles, such as polymer concentration variations in swollen P2VP domains. On the other hand, in dry and CH_3OH swollen films each layer was modeled by a simple box function, corresponding to a uniform scattering length density across the layer.

3. Results and Discussion

Assorted reflectivity data and calculated fits are displayed in Figure 2, and the corresponding sample SLD profiles are shown in Figure 3. The reflectivity curves in Figure 2 are vertically offset for clarity. The SLD profiles all share the same horizontal axis, with the substrate/film interface located at $z = 0$. The film is located in the half-space $z > 0$. The different block copolymer layers are labeled on curve 6 in Figure 3, with the P2VP domain next to the substrate designated as V1, the PS domain next to it as S1 and so on with higher numbers representing domains farther from the substrate. Since all specimens were 1.5 bilayers thick, they contain domains V1, S1, V2, and S2. The P2VP blocks wet the substrate surface while the PS blocks segregate to the film/air interface. The root-mean-square (rms) interfacial width is listed next to each interface in Figure 3.

The top curve in Figures 2 and 3 corresponds to the dry 50% triblock film. Since the diblock molecular weight is one-half the triblock molecular weight, the two polymers (and their blends) are effectively isomorphic in the dry state.[17,18] Accordingly, the dry state dimensions of all the films agreed to within ±5%, and all dry state data and fits were very similar to those of the 50% triblock film. In the dry state (curve 1 in Figure 2), the interference fringes primarily arose from the total film thickness because scattering from the PS/P2VP interfaces was weak due to low contrast. The dry state, root-mean-squared interfacial width between the PS and P2VP domains was 13 Å, with about a ±3 Å uncertainty due to the poor contrast.

Curves 2 through 6 in Figures 2 and 3 correspond to swollen films containing 100%, 80%, 50%, 20%, and 0% triblock. In the reflectivity data for swollen triblock-containing films in Figure 2, the sharp fringes at low q_z ($q_z < 0.05$ Å^{-1}) primarily correspond to the thickness of the V2 domain as indicated by the arrows on the 20% triblock data. Because in these films the interfaces surrounding S2 were sharp (less than 25 Å rms, Figure 3), the interference of their reflection with those surrounding the S1 domain dominated the low q_z regime. In contrast, in the pure diblock (curve 6 in Figure 2) the low q_z oscillations are absent because the interfaces around the S2 domain were much wider (about 70 Å rms) and therefore their reflection was weak. Above $q_z \approx 0.04$ Å^{-1}, a series of peaks corresponding to the width of the V1 domain are typically evident.

A native oxide layer about 10 Å thick is seen at the substrate/film interface for the top two SLD profiles in Figure 3 (dry and CH_3OH swollen samples). The oxide

Table 2. Domain Dimensions[a] in Å

sample		V1	S1	V2	S2
pure diblock	dry	108	195	195	108
	CD_3OD	340	220	863	218
20% triblock	dry	105	206	206	105
	CD_3OD	360	212	888	123
50% triblock	dry	115	202	201	115
	CD_3OD	362	212	834	120
80% triblock	dry	105	202	195	116
	CD_3OD	327	207	768	105
pure triblock	dry	112	186	191	91
	1st swelling CH_3OH	313	192	674	93
	5th swelling CH_3OH	343	190	742	92
	6th swelling CD_3OD	340	190	740	100

[a] Uncertainties in individual domain widths are less than ±5%.

layer is hard to distinguish in the other profiles because the scattering length density in the CD_3OD-swollen V1 domain is high, making the oxide appear as a small feature in the interface between the substrate and the V1 domain. The substrate rms roughness was close to 4 Å for all specimens. All of the SLD profiles in Figure 3 were generated from box function models; therefore, the SLD within each domain was assumed to be uniform except as modified by the presence of the left and right interfaces. The SLD profiles show a clear segregation of methanol to the V1 and V2 domains, which increased severalfold (~4 times) in width. The domain widths obtained from the SLD profiles are listed in Table 2. The dry state values were obtained after the sample has been swollen and redried at least once. For the pure triblock in the swollen state, three rows of entries are listed because we used this sample to examine the effects of repetitive swelling/drying cycles.

A consideration particular to a triblock-containing sample is whether some of the bridges relax when the film is swollen. To ascertain that the structure of a swollen film was static, we rescanned the first half of the reflectivity curve 4 h later (prior to drying) and confirmed that it reproduced the original scan. A pair of such reflectivity curves, obtained on the pure triblock sample, is plotted in part A of Figure 4. Any bridge relaxation would have to progress on a significantly slower time scale for it to be unnoticed in the measurements. Using the pure triblock sample, we also looked for effects of *drying and reswelling*. Part B of Figure 4 compares reflectivity data from the first and second swollen states. It is clear that the interference fringes have shifted to lower q_z. This shift reflects an increase in the total film thickness from 1270 to 1320 Å. Evidently, the process of drying and reswelling loosened some of the P2VP bridges so that the film swelled more during the second trial. A bridge may be especially susceptible if it were weakly anchored by its PS blocks or supported more than its share of stress due to a shorter P2VP block length or a large lateral displacement between the PS end anchors. Nevertheless, after the fourth swelling the reflectivity profiles started to superpose again as evident from part C of Figure 4. The lack of further change suggests that once the weakest and/or most strained bridges were loosened, the film stabilized to additional swelling/drying cycles. The SLD profiles corresponding to the first and fifth swollen states are displayed in Figure 5. The dimensions of S1 (~190 Å) and S2 (~90 Å) did not change, but V1 increased from about 310 to 340 Å and V2 from 670 to 740 Å. For the other films, only the initial swelling/

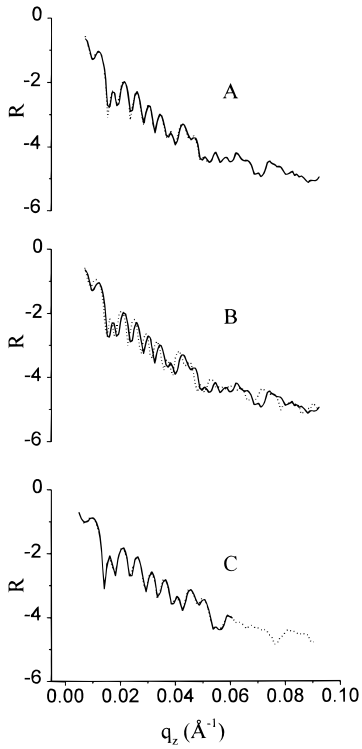

Figure 4. Reflectivity data for the pure triblock sample under CH_3OH. **(A)** Initial swelling of the film (—) with a rescan (- - -) 4 h later prior to drying. **(B)** Initial (—) and second (- - -) swelling of the film, with an intervening drying step. The peaks shift to lower q_z due to an increase in the width of the film, suggesting that some bridges were loosened by the drying/reswelling process. **(C)** Fourth (—) and fifth (- - -) swelling of the film, with an intervening drying. The data begin to superpose again.

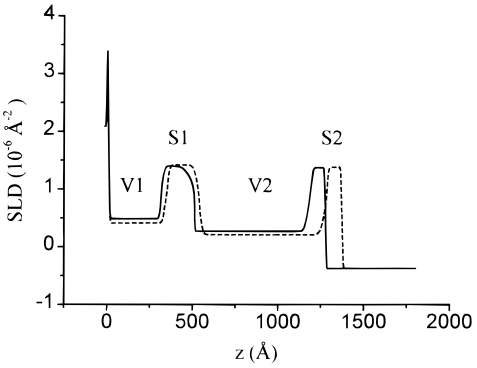

Figure 5. Scattering length density profiles for the pure triblock sample under CH_3OH in the initial (—) and fifth (- - -) swollen states.

drying cycle was performed. The swollen structure was always confirmed to be static over the time scale of measurement as in part A of Figure 4. All of the data and SLD profiles for swollen films in Figures 2 and 3 represent the initial swelling of the sample.

The S2 domain in the pure diblock sample manifested an apparent 2-fold increase in thickness (from 110 to 220 Å, Table 2) and a shift in its SLD toward the solvent value (curve 6 in Figure 3). Despite the altered appearance of diblock S2 domains in the swollen state, we have repeatedly shown[19] that after drying sharply defined S2 domains are recovered. Furthermore, swelling of the samples did not induce such changes in the diblock S1 domain or any of the PS domains in the triblock-containing films (Figure 3). The changes in the diblock

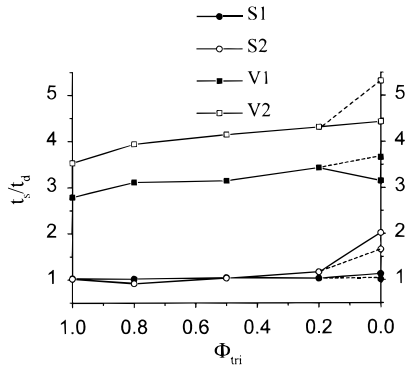

Figure 6. Ratio of swollen to dry domain width, t_s/t_d, as a function of triblock volume fraction. In the pure diblock limit, the solid lines connect to data from the 78K diblock sample of the present study, while the dashed lines connect to data from a 76K diblock sample.[19] For the PS domains, t_s/t_d gauges their deformation from a planar state (a t_s/t_d of 1 indicates an undeformed PS domain). Please see text for further discussion.

S2 domain arise from its deformation (e.g., buckling, bending) due to osmotic repulsions acting between solvated P2VP blocks. The neutron reflectivity measurement averages laterally over any such distortions, causing the S2 domain to appear thicker, and its SLD shifted toward the solvent value. Additionally, the ability of diblock films to withstand repetitive swelling/drying cycles in the absence of native bridging has been attributed[19] to the reinforcing action of microstructural defects[20,21] that interconnect the undissolved PS layers of the films. Unlike the diblock S2 domain, the S1 domain is not deformed in the swollen state because bridges between it and the silicon wafer, formed by adsorption of P2VP blocks to the substrate, constrain it to remain flat and topologically conformal with respect to the substrate surface. By keeping the S1 domain flat, all bridges can be comparably stretched so elastic penalties are minimized. In triblock-containing films, the presence of bridges in the V2 domain maintains the S2 domain conformal with respect to S1, so that S2 also remains flat and sharply defined (curves 2−5 in Figure 3). Evidently, even 20% triblock fraction is effective in suppressing the deformation of the S2 domain.

The effects of bridging on film structure can be summarized in a plot of the swelling ratio t_s/t_d, where t_s and t_d are the widths of a domain in the swollen and dry states. Such a plot is shown in Figure 6 as a function of triblock content. We emphasize that the "swollen" width of the PS domains reflects their deformation from a planar shape rather than dissolution by methanol. For instance, a PS domain that remained flat in the swollen state would possess $t_s/t_d \approx 1$ while one that buckled and became distorted would appear wider with $t_s/t_d > 1$. Accordingly, since the S1 domain was not deformed in the presence of solvent its t_s/t_d remained close to unity at all compositions. For the S2 domain, t_s/t_d remained close to unity as long as some triblock was present, affirming that the triblock bridges maintain the S2 domain aligned with respect to S1. Only initial swelling data are considered in Figure 6, and they were obtained with CD_3OD as the solvent except for the 100% triblock film for which CH_3OH was used. We did not find any evidence of isotopic effects on swollen domain dimensions (cf. fifth and sixth swelling trials of the 100% triblock sample in Table 2).

In the pure diblock sample, the V2 domain consists of opposing P2VP polymer brushes,[22] one tethered to the S1 and the other to the S2 domain. We expect that the brush tethered to the S2 domain should be less stretched because the repulsive interactions between its P2VP blocks have been partially relieved by the deformation of the S2 domain. To illustrate this effect two sets of data are displayed for the pure diblock case in Figure 6—one representing the 78K PS−P2VP sample of the present study (connected by solid lines) while the other was a 76K symmetric PS−P2VP film examined under identical conditions[19] (connected by dashed lines). The reason for including the 76K data is that its S2 domain was less distorted, so that the attached P2VP brush should be more strongly stretched. The lesser distortion of S2 in the 76K film is reflected in its lower t_s/t_d ratio, which was 1.7 compared to 2.0 for the 78K diblock. In addition, a clear upturn in the V2 t_s/t_d curve near the pure diblock limit is observed with the 76K diblock data. Since S2 was less deformed in the 76K sample, the P2VP brush tethered to it should be more strongly stretched, leading to a greater V2 t_s/t_d and the upturn in the pure diblock limit. The reason the S2 domain was more deformed in the 78K film than in the 76K sample, despite near equivalence in molecular weight and sample preparation, is not clear at present.

The t_s/t_d ratio is about 25% less for the V1 domain than for V2 because of adsorption of P2VP segments to the substrate. The adsorption leaves fewer segments per chain available for swelling. Both the V1 and V2 swelling ratios increase with the volume fraction of diblock. For the V2 domain, t_s/t_d rises from 3.5 for 100% triblock to a maximum of 5.3 for the pure 76K diblock, about a 50% expansion. A 27% expansion is obtained using the 78K diblock data. In our opinion, the effects of triblock content on film swelling are better captured in the pure diblock limit by the 76K diblock than the 78K diblock data. This is because the 76K sample was less affected by the additional influence of S2 deformation on the swollen dimension of the V2 domain.

The experimentally measured expansion of V2 t_s/t_d on passing from pure triblock to pure diblock can be compared to a ∼35% maximum increase predicted by analytical self-consistent mean field (ASCMF) theory.[6] The theoretical increase is predicted to occur as the fraction of bridging chains decreases from 1 to 0. The 27% expansion obtained with the 78K diblock data is consistent with the theoretically expected range of swelling. From Figure 5 in ref 6, a 27% expansion would indicate that ∼70% of the chains are involved in bridging in the pure triblock sample. However, as noted above, we believe that the 50% expansion derived using the 76K diblock limit is more appropriate for considering the influence of blend composition on film swelling. In that case, our data suggest that the ASCMF theory underestimates the effects of bridging. Indeed, there are several reasons why the ASCMF prediction of 35% maximum expansion may be less than the experimentally observed value of 50%. The experimental system consists of chains that are not perfectly monodisperse. Shorter, more stressed bridges will dominate the swelling of triblock-containing samples and impose stricter limits on their expansion. In addition, lateral displacements of bridge anchors and the resultant "nonperpendicular" orientation of a bridge with respect to the PS/P2VP interfaces will result in greater stress at a given domain width. Both polydispersity and lateral displacement of bridge anchors serve to limit the swelling of V2 in triblock films, enhancing the experimentally observed

difference between triblock-containing and pure diblock samples. The ASCMF treatment[6] does not include these effects, so a more modest prediction of the difference between triblock and diblock swelling is anticipated. Regardless, comparison of the present data to theoretical predictions is complicated by the deformation of the diblock S2 domain and the accompanying effect on the width of V2.

A swollen domain spanned by bridges in a lamellar block copolymer film is similar to the situation of two parallel, planar surfaces spanned by end-adsorbed, telechelic polymers. For the telechelic chain system, the distance between the surfaces determines the ratio of bridging to looping chains. Misra et al.[23] performed Monte Carlo simulations in which the bridging fraction of irreversibly adsorbing telechelic polymers was obtained at different surface separations. The simulations indicate a relationship between surface separation and bridging fraction that is qualitatively in agreement with that between V2 t_s/t_d and triblock content in Figure 6, especially if the 76K data are taken as the pure diblock limit. In particular, the rise in V2 dimension (corresponding to greater separation between adsorbing surfaces in the simulations) is weaker at intermediate values of triblock content (telechelic chain bridging fraction) than at the extremes.

While a higher triblock content of a sample should correlate with an increase in bridging, the detailed relationship between the two parameters is not clear. For a pure melt of polystyrene−polyisoprene−polystyrene triblock copolymer, a recent dielectric relaxation study by Watanabe[24] estimated that ∼40% of middle blocks form single chain bridges, in agreement with theoretical calculations.[25] While no estimates are available regarding the variation in bridging when diblock of half the triblock molecular weight is added, one may speculate that the number of bridges should vary as $\sim\phi + \phi^2$, where ϕ is the triblock volume fraction. The linear term in ϕ represents the single chain contribution while the quadratic term refers to entangled loops since two loops must "meet" in order to form a bridge. Unfortunately, the present data do not lend themselves to a verification of such a relationship between ϕ and the number density of bridges since the bridge density is unknown.

Additional details about the swollen film structure can be deduced if the a priori assumption of a uniform SLD within the PS and P2VP domains is relaxed. Accordingly, a cubic spline expansion[16] of the SLD was used to generate refinements to the box model profiles. The indicated improvements were then incorporated into the structural models by using simple polynomials instead of box functions to represent the various sample layers.[11] The final SLD profiles for 100%, 20%, and 0% triblock fractions are plotted in Figure 7. The improvements in χ^2,[2,15] relative to box model fits, are indicated in the figure. The 20% curve is assembled directly from a cubic spline expansion, while the other two are structural model profiles altered to incorporate features suggested by cubic spline fits. Since the scattering length densities of PS (1.4×10^{-6} Å^{-2}) and P2VP (2.0×10^{-6} Å^{-2}) are less than that of CD_3OD (5.8×10^{-6} Å^{-2}), regions of lower SLD within a domain signify richer polymer content.

Several of the novel features were reproducible for all samples examined and resulted in marked improvements to the reflectivity fits. In the triblock samples

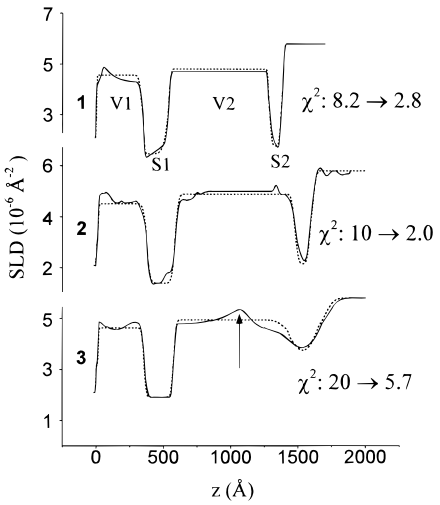

Figure 7. Solid (—) SLD profiles account for intradomain polymer concentration variations in films swollen with CD_3OD. Curves 1 and 3 are structural models incorporating features suggested by cubic spline fits, while curve 2 is a cubic spline SLD. The improvements in χ^2 over the corresponding box models are indicated. In each case, the predecessor box model SLD profile is plotted with a dashed line: **(1)** 100% triblock sample, **(2)** 20% triblock sample, and **(3)** 0% triblock sample. The arrow on profile 3 marks the meeting point of the opposing brushes in the diblock V2 domain.

(first and second curves in Figure 7), the SLD in the S1 domain was observed to increase with *z*. The increase indicates a deficiency of PS on the high-*z* side of S1. This feature reflects a pull-out of PS anchor blocks into the V2 domain by the tension in P2VP bridges (or entangled P2VP loops) during swelling. Therefore, as previously illustrated by the data in Figures 4 and 5, a bridge relaxation process occurred. PS anchors can be yanked from the S2 domain as well. The vacancies thus created would become filled with solvent and should be at least partly responsible for the shift of the S2 domains' SLD toward the solvent value. No quantifiable deficiency of PS on the *low-z* side of S1 was detected, suggesting that few PS anchors were pulled out into the V1 domain. We note that a bridge in V1 can relax by desorbing from the substrate, so that pull-out of PS anchors is not necessary. If desorption is the primary relaxation process in V1, those bridges bearing the greatest stress loads could relax without any disruption to the S1 domain.

In the pure diblock sample (third curve in Figure 7), the opposing P2VP brushes in the V2 domain come together at the point indicated by the arrow. This point corresponds to a minimum in the polymer volume fraction of about 10%. The width of the left brush is 500 Å whereas the right brush extends 360 Å. The lesser extent of the right brush is consistent with our earlier argument regarding partial relief of its stretching due to deformation of the S2 domain. While the nonuniform SLD profile in the V2 domain of the pure diblock film reflects the presence of two opposing polymer brushes, in triblock-containing films good fits were obtained with an essentially uniform V2 profile (even if just 20% triblock was present). The uniform SLD in triblock-containing V2 domains may arise because (1) both single chain and entangled loop bridges tend to distribute their segments evenly across the width of the V2 domain and (2) the tension present in bridges pulls the S1 and S2 domains closer, thus compressing the V2 domain and smoothing out varia-

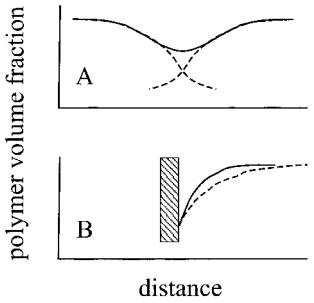

Figure 8. Effect of compressing a polymer brush against (A) another brush and (B) against an impenetrable wall. In part A, the individual brushes (- - -) can interpenetrate, leading to a total concentration profile (—) that is more uniform. In part B, the impenetrable barrier maintains a depletion zone next to the wall, although the profile (—) can become distorted from its uncompressed state (- - -).

tions in P2VP concentration. The even distribution of segments in single chain bridges has been confirmed by Monte Carlo simulations,[23] while smoothed total polymer concentration profiles for a pair of opposing, compressed brushes were seen in Monte Carlo[26] and molecular dynamics studies.[27] The simulations[26,27] also indicate that compressed brushes interpenetrate, suggesting that smoothed profiles are more a result of interpenetration rather than distortion of individual brush profiles. This is schematically illustrated in part A of Figure 8.

The SLD in the V1 domain next to the substrate is less than the pure CD_3OD value of 5.8×10^{-6} Å^{-2}. This is expected because adsorbed P2VP segments lower the SLD in this region. Additionally, the SLD is nonuniform with a minimum (maximum) in polymer content (SLD) near the substrate surface. These variations point to an interesting observation. In particular, concentration variations are not as effectively suppressed in V1 as they are in V2. Since in V1 the swollen P2VP chains are pushed against the impenetrable surface of the substrate, their concentration profile cannot be smoothed by the interpenetration mechanism portrayed in part A of Figure 8. Rather, the impenetrable barrier causes a depletion zone in the polymer concentration profile. Therefore, in agreement with the SLD profiles in Figure 7, we expect that the V1 concentration profile becomes distorted as illustrated in part B of Figure 8.

4. Summary

Lamellar block copolymer films consisting of a blend of 78 000 g/mol poly(styrene-*b*-2-vinylpyridine) (PS−P2VP) diblock and a 159 000 g/mol PS−P2VP−PS triblock were swollen with methanol. Methanol solvates P2VP but is a nonsolvent for PS. One and a half bilayer thick films containing 100%, 80%, 50%, 20%, and 0% triblock were investigated. Neutron reflectivity was used to characterize the structure of dry and methanol-swollen films. The dry state dimensions of the samples were similar within ±5% for all blend compositions, in accordance with the morphological equivalence of triblocks and diblocks of half the triblock size.[17,18]

In swollen films, a prominent segregation of methanol into the P2VP domains occurred. While swelling and drying did not disrupt the lamellar morphology of the samples, triblock-containing films did exhibit a limited degree of bridge pullout. A decrease in triblock content led to increased swelling of the film. For example, an internal P2VP domain in a pure diblock film swelled by up to 50% more than in a pure triblock sample. Furthermore, even for just 20% triblock content by volume, the presence of bridges maintained the PS domains planar and parallel to the substrate in the swollen state. In swollen triblock-containing films, the polymer concentration profile appeared uniform in internal P2VP domains. In contrast, in the pure diblock film the profile exhibited variations consistent with a pair of opposing P2VP brushes.

Acknowledgment. Financial support for this research was provided by a graduate NSF fellowship (R.L.) and the Earl E. Bakken Endowment Funds at the University of Minnesota. Part of this work was also supported by the Center for Interfacial Engineering (CIE), an NSF engineering research center at the University of Minnesota.

References and Notes

(1) Riess, G.; Hurtrez, G.; Bahadur, P. In *Encyclopedia of Polymer Science and Engineering*, 2nd ed.; John Wiley & Sons: New York, 1985; Vol. 2.

(2) Dai, L.; Toprakcioglu, C. *Macromolecules* **1992**, *25*, 6000. *Europhys. Lett.* **1991**, *16*, 331.

(3) Milner, S. T.; Witten, T. A. *Macromolecules* **1992**, *25*, 5495. Tang, W. H.; Witten, T. A. *Macromolecules* **1996**, *29*, 4412.

(4) Mayes, A. M.; Olvera de la Cruz, M. *J. Chem. Phys.* **1989**, *91*, 7228.

(5) Gehlsen, M. D.; Almdal, K.; Bates, F. S. *Macromolecules* **1992**, *25*, 939.

(6) Zhulina, E. B.; Halperin A. *Macromolecules* **1992**, *25*, 5730.

(7) Halperin, A.; Zhulina, E. B. *Europhys. Lett.* **1991**, *16*, 337.

(8) Skoulios, A. E.; Tsouladze, G.; Franta, E. *J. Polym. Sci. C* **1963**, *4*, 507.

(9) Folkes, M. J.; Keller, H. H. *J. Polym. Sci.: Polym. Phys.* **1976**, *14*, 833. Folkes, M. J.; Keller, H. H.; Odell, J. A. *J. Polym. Sci.: Polym. Phys.* **1976**, *14*, 847.

(10) Reynders, K.; Mischenko, N.; Mortensen, K.; Overbergh, N.; Reynaers, H. *Macromolecules* **1995**, *28*, 8699.

(11) Levicky, R. Ph.D. Dissertation. University of Minnesota, 1996.

(12) Coulon, G.; Russell, T. P.; Deline, V. R.; Green, P. F. *Macromolecules* **1989**, *22*, 2581.

(13) Parratt, L. G. *Phys. Rev.* **1954**, *95*, 359.

(14) Russell, T. P. *Mater. Sci. Rep.* **1990**, *5*, 171.

(15) $\chi^2 = P^{-1} \sum [(R_{i\,\mathrm{exp}} - R_{i\,\mathrm{cal}})^2/\delta R_i^2]$ where P is the number of data points, $R_{i\,\mathrm{exp}}$ is the experimentally measured reflectivity for data point i with standard deviation δR_i, and $R_{i\,\mathrm{cal}}$ is the theoretically calculated reflectivity.

(16) Pedersen, J. S. *J. Appl. Crystallogr.* **1992**, *25*, 129. Pedersen, J. S.; Hamley, I. W. *J. Appl. Crystallogr.* **1994**, *27*, 36.

(17) Matsushita, Y.; Nomura, M.; Watanabe, J.; Mogi, Y.; Noda, I.; Imai, M. *Macromolecules* **1995**, *28*, 6007.

(18) Hadziioannou, G.; Skoulios, A. *Macromolecules* **1982**, *15*, 258.

(19) Levicky, R.; Koneripalli, N.; Tirrell, M.; Satija, S. K.; Gallagher, P. D.; Ankner, J. F.; Kulasekere, R.; Kaiser, H. Submitted for publication in *Macromolecules*.

(20) Liu, Y.; Rafailovich, M. H.; Sokolov, J.; Schwarz, S. A.; Bahal, S. *Macromolecules* **1996**, *29*, 899.

(21) Carvalho, B. L.; Thomas, E. L. *Phys. Rev. Lett.* **1994**, *73*, 3321.

(22) Alexander, S. *J. Phys. (Paris)* **1977**, *38*, 983. de Gennes, P. G. *Macromolecules* **1980**, *13*, 1069.

(23) Misra, S.; Mattice, W. L. *Macromolecules* **1994**, *27*, 2058.

(24) Watanabe, H. *Macromolecules* **1995**, *28*, 5006.

(25) Matsen, M. W.; Schick, M. *Macromolecules* **1994**, *27*, 187.

(26) Dickman, R.; Hong, D. C. *J. Chem. Phys.* **1991**, *95*, 4650.

(27) Murat, M.; Grest, G. S. *Phys. Rev. Lett.* **1989**, *63*, 1074.

MA9716185